Arabian Journal of Geosciences (2021) 14:2243
https://doi.org/10.1007/s12517-021-08610-1

ORIGINAL PAPER

Spatial modeling of flood susceptibility using machine learning algorithms

Modeste Meliho[1] · Abdellatif Khattabi[2] · Joseph Asinyo[3]

Received: 6 May 2021 / Accepted: 13 October 2021

Abstract

Floods constitute one of the most devastating and destructive natural forces in the world. They have a considerable impact on the economy and can result in significant loss of life. Several strategies, including studies by advanced data analysis methods, have been adopted to curb this phenomenon and ultimately limit the accompanying damage. In this study, four supervised models based on machine learning (ML) algorithms were used to map flood vulnerability in the Souss watershed located in southern Morocco. They include random forest, x-gradient boost, k-nearest neighbors and artificial neural network. Thirteen predisposing factors including aspect, curvature, digital elevation model (DEM), distance to rivers, drainage density, flow accumulation, flow direction, geology, land use, rainfall, slope, soil type, and topographic wetness index (TWI) were selected as inputs to achieve this. Four different models were developed for each ML algorithm based on variable selection and one-hot encoding. Overall, all the models of the four algorithms have an AUC score above 80% for the testing data, which means that they all performed very well. The ranking of the ML algorithms used by considering only the most efficient model of each algorithm is as follows: KNN (98.6%), RF (98.1%), XGB (97.2%), and NNET (95.9%). Finally, all the models were overlaid to identify points of agreement or disagreement. This study provides evidence of ML models being successful in mapping flood vulnerability. These findings can be beneficial, serving as an important resource in mitigating the impacts of floods in the highlighted vulnerable areas presented in the flood vulnerability maps.

Keywords Flood spatial modeling · Machine learning · Souss watershed · Morocco

Introduction

The threat posed by natural disasters is significant to both humans and wildlife, with the associated damages extending from the destruction of property to the loss of life (Samanta et al. 2018). The economic losses associated with these events have been estimated to be as high as 40% (Li-Hua and Jia 2010). Owing to the frequency and considerable losses associated with them, floods are considered one of the most destructive natural disasters (Doocy et al. 2013). Their impacts are all too apparent, affecting nearly 100 million people worldwide between 2000 and 2008 (Opolot 2013). Floods often occur following heavy rainfall. They cause riverbanks to overflow, leading to the destruction and damage of infrastructure. In addition, they disrupt both the natural ecosystem and the overall functioning of society.

The frequency and severity of flooding in Morocco are likely to increase due to global warming, urbanization, poor watershed management, deforestation, and land use changes. It is therefore incumbent upon the government and researchers to identify and implement mitigation strategies to reduce the damage caused by flooding. One approach is using spatial delineation of flood vulnerability as the basis for an early warning system. This makes it possible to delineate areas that are shown to be susceptible to flooding so that appropriate actions can be taken to reduce their impact (Zkhiri et al. 2016).

Responsible Editor: Biswajeet Pradhan

✉ Modeste Meliho
modestemeliho@yahoo.fr

[1] Association Marocaine des Sciences Régionales (AMSR), Avenue Allal El Fassi Madinat Al Irfane, B.P 6215, Rabat, Morocco

[2] Ecole Nationale Forestière d'Ingénieurs, BP 511 Tabriquet, 11000 Sale, Morocco

[3] Université Mundiapolis de Casablanca, 380 Boulevard Brahim Roudani, Casablanca, Morocco

Published online: 30 October 2021

Spatial analysis techniques relying on geographic information systems (GIS), remote sensing (RS), and statistics have proven to be of great value in mapping flood susceptibility. They are used extensively by researchers in identifying, assessing, and monitoring flood hazards (Pradhan 2009; Pradhan et al. 2010). Combinations of hydrological models such as SWAT (Jayakrishnan et al. 2005) and HYDROTEL (Jutras et al. 2009) with RS and GIS have been employed to obtain data and analyze the spatial parameters of flooding. Based on their significantly lower processing time and ease of understanding, statistical techniques have been routinely used and are often preferred over complex approaches such as machine learning. The most comprehensive statistical techniques used for flood vulnerability mapping can be divided into two groups: bivariate statistical analysis and multivariate statistical analysis (Diakakis et al. 2016; Al-Juaidi et al. 2018; Ayalew and Yamagishi 2005; Tien Bui et al. 2019a, b; Tehrany et al. 2019; Al-Abadi and Al-Najar 2020).

Breakthroughs in ML techniques in recent years have significantly improved spatial analysis and provided better flood vulnerability assessment, which has been crucial in overcoming the limitations of conventional flood modeling and consequently improving their accuracy (Xu and Li 2002; Wang et al. 2015). These models are often lacking in their ability to capture the physics in mathematical terms, but they remain very popular. This is made possible by the numerical formulation of the nonlinearity of the flooding that is independent of the underlying processes, thanks to the use of data of past flood events thus maintaining ease of use with low computing cost (Hosseiny et al. 2020; Mosavi et al. 2018). There have been many successful studies using ML models. One of the most popular methods for flood prediction is the artificial neural network (ANN) (Shu and Burn 2004; Seckin et al. 2013; Campolo et al. 2003; Kim et al. 2016; Jahangir et al. 2019). Alternatively, other models including support vector machine (Chapi et al. 2017; Ahmadlou et al. 2018), random forest (Tehrany et al. 2019; Tehrany et al. 2014), logistic regression (Pradhan et al. 2010), and adaptive neuro-fuzzy inference system (ANFIS) (Tehrany et al. 2015) have been used for flood risk prediction.

Extensive work is needed to improve physical and statistical models due to their inaccuracy, robustness, and operational complexity and cost (Mosavi et al. 2017). Such limitations justify the use of advanced data-driven approaches such as ML modeling, which can quantify the non-linearity of flooding based solely on historical data without the need for understanding the inherent physical processes involved. ML techniques allow for easier implementation at low computational cost, along with rapid training, validation, testing, and evaluation. They offer a high performance compared to physical models and are relatively less complex. Thus, the steady progress of these techniques over the past two decades has led to better results in terms of their suitability for flood prediction (Mekanik et al. 2013; Mosavi et al. 2017). Indeed, Abbot and Marohasy (2017) found ML models to be of higher accuracy when compared to conventional methods in a recent study.

Floods constitute the most important natural hazards in Morocco in terms of their impact on the economy and the population. The south of Morocco represents the region most vulnerable to flooding. It encompasses the High Atlas watersheds of N'Fis, Rheraya, Ourika, Zat, and R'dat located upstream of the city of Marrakech. These represent areas where flooding has occurred in the past, significantly affecting the population (Tien Bui et al. 2016).

Studies have been conducted on soil erosion and dam siltation in the Souss watershed, which is known to be vulnerable to flooding (Hssaisoune et al. 2016; Elmouden et al. 2016; El Morjani et al. 2016). However, it is clear from the literature that the limited studies related to flood risk assessment in this region have only employed GIS, remote sensing, and multicriteria analysis techniques (El Morjani et al. 2016). Despite the demonstrated ability of ML algorithms in terms of accuracy compared to traditional methods in predicting natural hazards, their application in predicting flood susceptibility is either limited or absent in Morocco. Thus, the purpose of this research is to use models based on random forest (RF), extreme gradient boost (XGB), K-nearest neighbors (KNN), and artificial neural network (ANN) algorithms to generate flood susceptibility maps and to compare their performance results. Specifically, the objectives of this study include (i) identifying the most significant factors influencing flooding for modeling, (ii) implementing the ML models to produce flood susceptibility maps, (iii) comparing the models in terms of predictive accuracy, and (iv) comparing the models' flood susceptibility maps. This study will show that ML algorithms can be successfully used for flood susceptibility mapping and will be beneficial for the strategic planning and management of floods in the Souss watershed.

Materials and methods

Study area

The Souss watershed, which spans an area of about 17,000 km^2, is located in southwest Morocco. It is bounded to the north by the High Atlas Mountains, to the south and east by the Anti-Atlas Mountains, to the east by the Siroua massif, and to the west by the Atlantic Ocean (Fig. 1). Numerous devastating floods have been recorded over the past decade in the watershed (El Morjani et al. 2016), with the risk of flooding increasing over time due to population growth driving uncontrolled urbanization and deforestation.

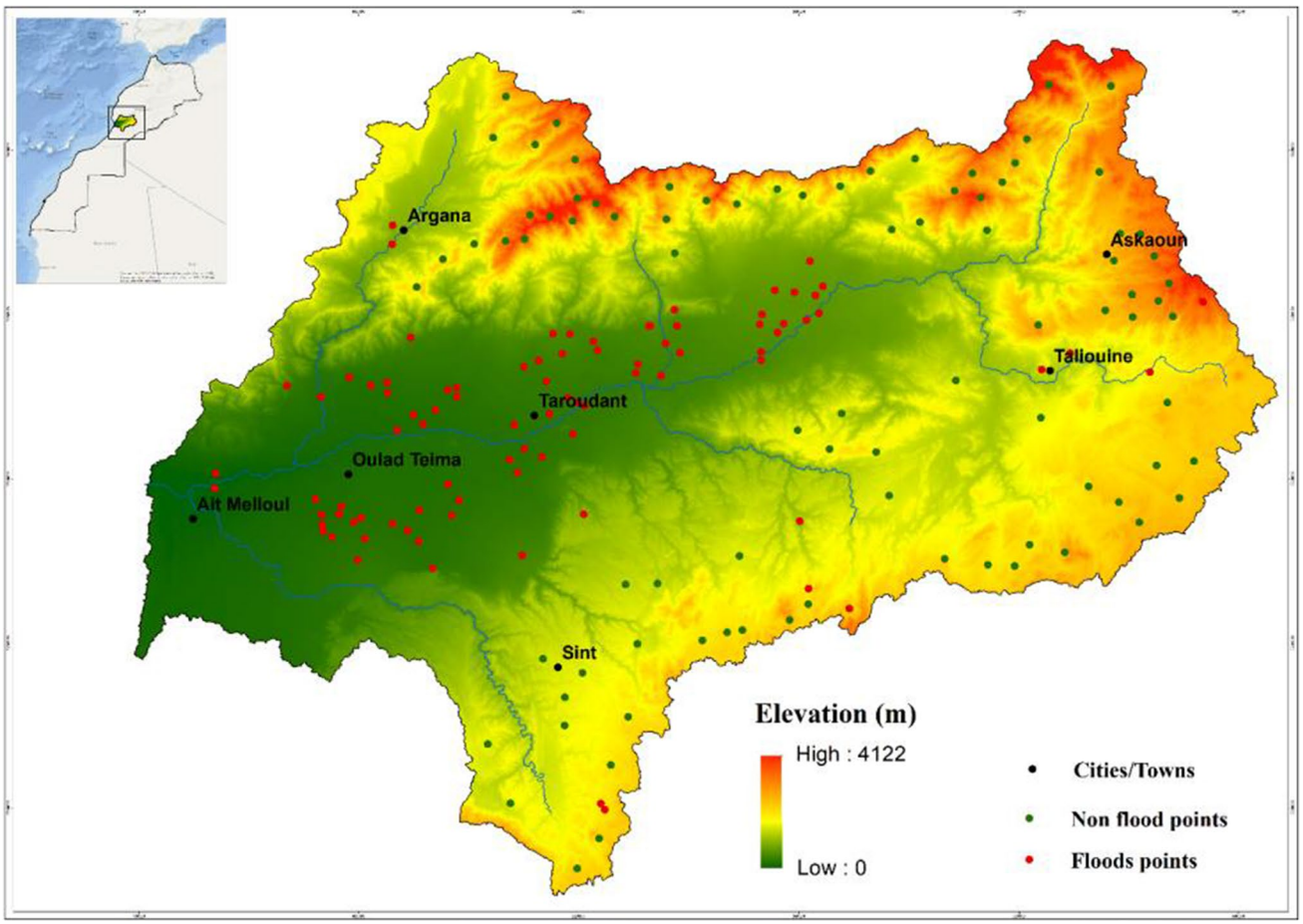

Fig. 1 Location of the study area and floods inventory

Floods inventory and conditioning factors analysis

Access to data is considered the most difficult aspect of this type of study (Carrara et al. 1999). However, thanks to the Agence du Bassin Hydraulique du Souss-Massa (ABHSM), the data for the inventory of flooding points in the watershed was made available. In total, 87 historical flood points were provided by ABHSM. Another 87 non-flood points were chosen randomly from areas with slopes greater than 50% (Fig. 1). The assumption is that if the slope is greater than 50%, they are non-flood points, as all 87 flood points are on a slope less than 50%.

Many flood predisposing factors have been selected, looking into the literature. Those identified in this study were digital elevation model (DEM), aspect, curvature, distance to rivers, drainage density, flow accumulation, flow direction, geology, land use, precipitation, slope, soil type, and topographic moisture index (Figs. 2 and 3). A 30-m-resolution DEM published in 2016 and downloaded from the ASTER GDEM website (https://asterweb.jpl.nasa.gov/gdem.asp) was used (Fig. 2b). Subsequently, aspect, curvature, distance to rivers, drainage density, flow accumulation, flow direction, and slope were derived from the DEM. The geology factor was extracted from the 1956 geological map of the Moroccan High Atlas while the land cover map was derived from the High Commission for Water and Forests and the Fight against Desertification of Morocco forest domain map and the 2018 global land cover (Buchhorn et al. 2018). Soil type was derived from the 2012 harmonized FAO soil database (FAO 2012), while rainfall data for the period between 1986 and 2019 was provided by ABHSM.

Both the amount of rainfall and the rate of sunshine are influenced by aspect (Tehrany et al. 2019). A classification of the aspect map resulted in eight classes: N, NE, E, SE, S, SW, W, and NW (Fig. 3a). Curvature is one of the most important factors influencing surface runoff and water accumulation (Fig. 2a) by controlling the flow of surface water (Al-Abadi and Al-Najar 2020). While positive and negative curvature values signal concavity and convexity of the surface, respectively, a zero value indicates flatness (Meliho et al. 2018). The susceptibility of an area to flooding is indicated by the distance to rivers (Fig. 2c). Indeed,

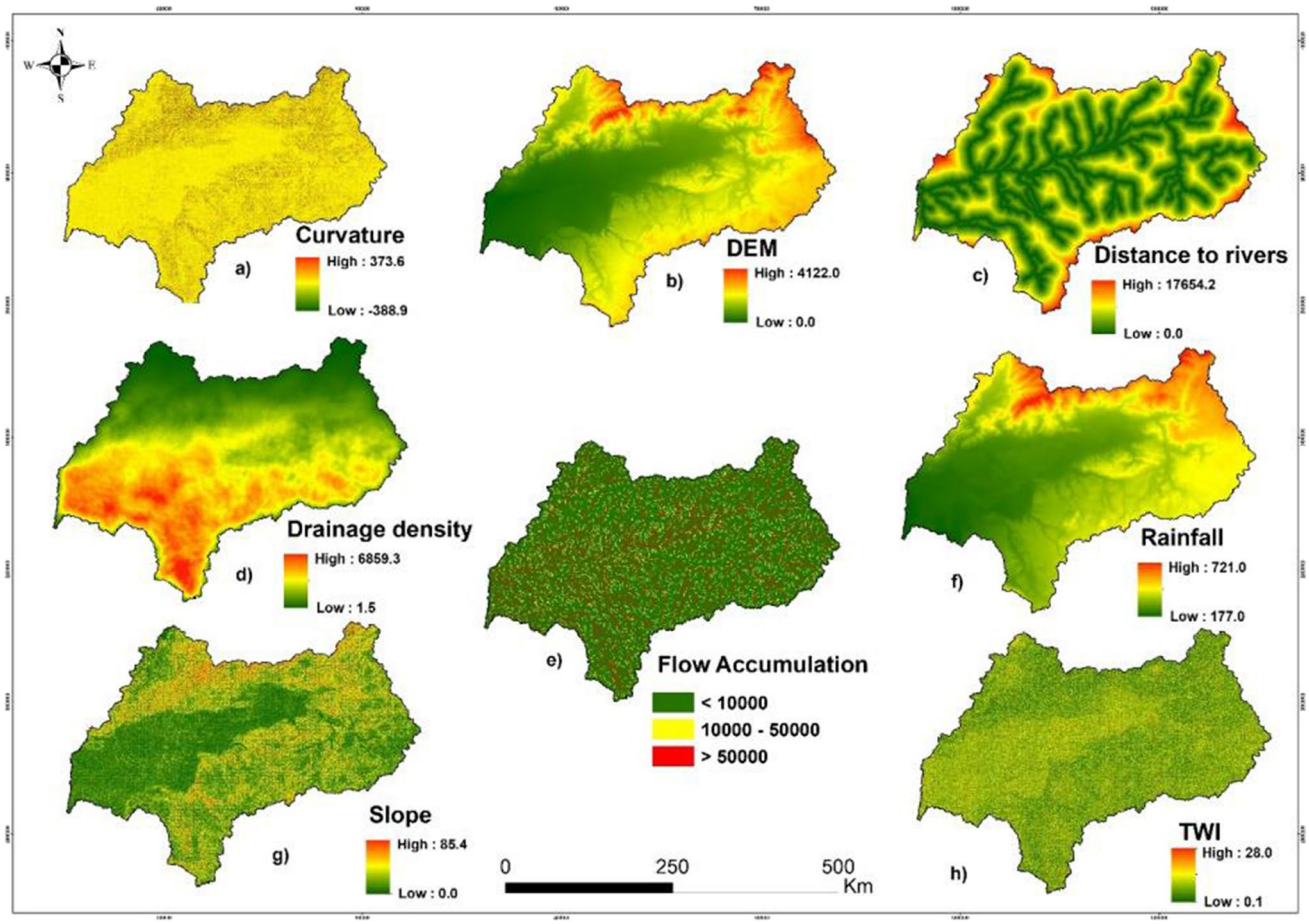

Fig. 2 Predisposing factors used as numerical variables in floods susceptibility modeling

the closer it is, the more likely it is to flood (Tehrany et al. 2019). Drainage density is correlated with the large volume of accumulated water flow (Fig. 2d) and is often a contributing factor to flood events (Jahangir et al. 2019).

Slope gradient (Fig. 2g) is connected with flooding as it directly influences surface runoff, thus exacerbating these disastrous events (Al-Abadi and Al-Najar 2020). Flood susceptibility is greater the lower the slope angle of an area (Tien Bui et al. 2019a, b). TWI provides a basis for establishing the variation in wetness in a watershed (Fig. 2h). It makes it possible to predict the amount of water accumulated at any time, indicating the receding pattern of gravitational forces (Lee et al. 2017). Thus, there is a greater vulnerability to flooding the higher the TWI of an area (Khosravi et al. 2019). TWI is calculated as follows:

$TWI = \ln(As / \tan\beta)$, where As is the specific watershed area (m) and β is the slope gradient (°).

The most important flood conditioning factor is considered to be rainfall (Fig. 2f), with flooding often occurring following heavy rain events (Cao et al. 2016). Land use type (Fig. 3d) directly or indirectly influences the creation of surface runoff, penetration, and evapotranspiration, which leads to flooding (Khosravi et al. 2018). Soil (Fig. 3e) is one of the most important factors, as soil type greatly determines infiltration and thus the amount of runoff that results in flooding).

Flow direction (Fig. 3b) is critical in estimating flow accumulation for a given area. It can be classified into eight directions: east (E), southeast (SE), south (S), southwest (SW), west (W), northwest (NW), north (N), and northeast (NE). Knowledge of flow direction helps compare areas based on the accumulation of water (Jahangir 2019). How prone an area is to the accumulation of water is crucial to its susceptibility to flooding. The flow accumulation capacity of an area helps identify areas with a high likelihood of accumulating water. Accumulated flow is the total amount of water flowing along the slope in the outlet matrix cells, with higher values indicating areas of higher flood risk (Kazakis et al. 2015). Geology (Fig. 3c), which influences the permeability of rocks, is considered an important factor in determining the likelihood of flood events (Khosravi et al. 2019). Effectively, resistant rocks and highly permeable soils exhibit channels with low density (Srivastava et al. 2014).

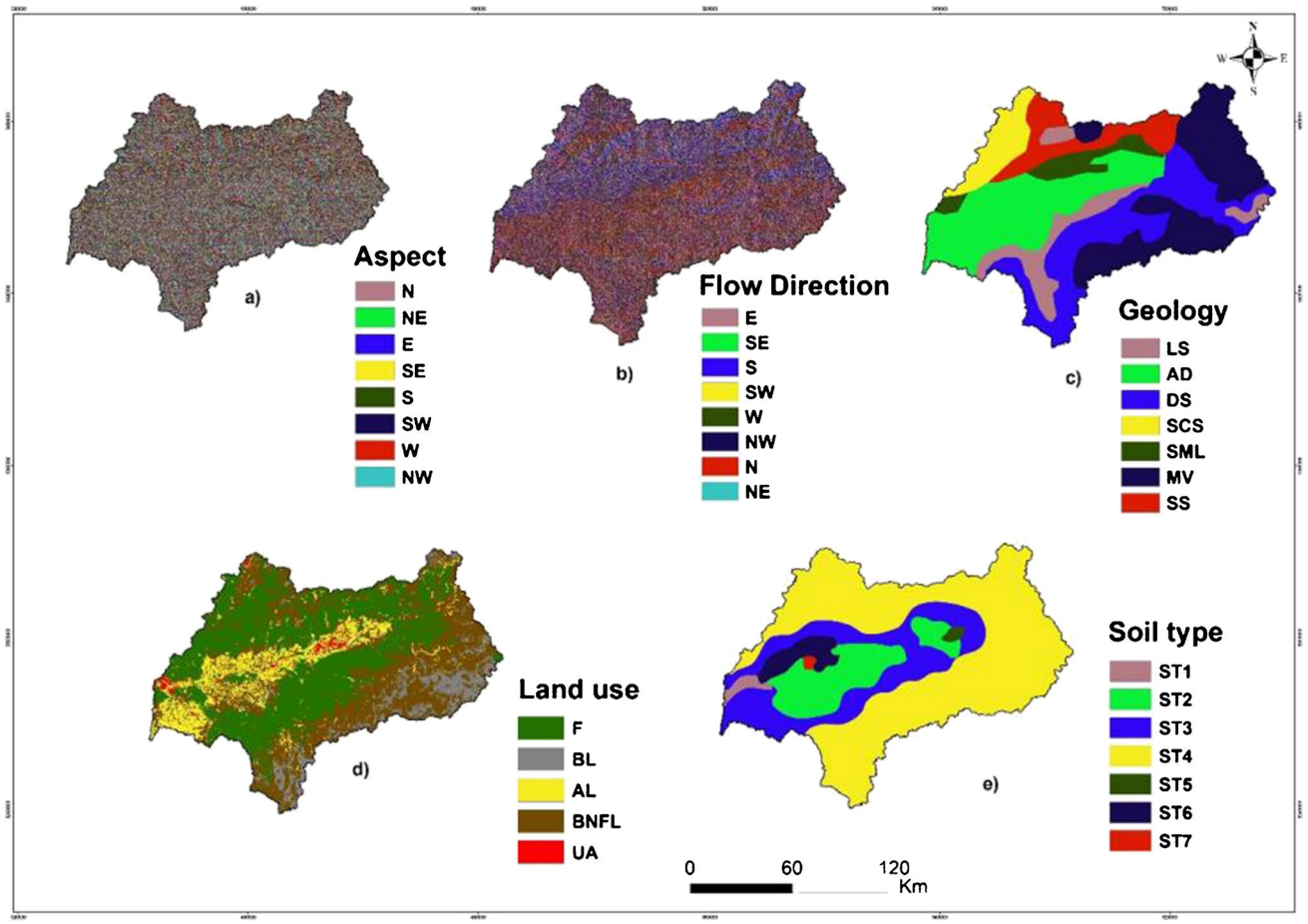

Fig. 3 Categorical variables (ST1, poorly evolved soils with inclusion of raw minerals; ST2, calcimagnesic soils with inclusion of poorly evolved soils; ST3, poorly evolved soils of fluvial input; ST4, isohumic soils; ST5, poorly evolved soils with inclusion of iron sesquioxide soils; ST6, Vertisols with inclusion of isohumic soils; ST7, sesquioxide soils with calcimagnesium inclusion; LS, limestone and shale; AD, alluvium deposits; DS, dolomites and silts; SCS, sandstone and clay silts; SML, silt and marl-limestone; MV, metamorphic and volcanic rocks; SS, shale and sandstone; F, forest; BS, bare soil; AL, agricultural land; BNFL, bare non-forest land; UA, urban area)

Susceptibility modeling

Understanding and solving problems using data-driven technologies such as ML have made great strides in recent years. This has greatly benefited many research areas including geography and hydrology. The increase in computing power and the ability to collect and process large data have made this possible. ML models provide robust ways of estimating flood vulnerability by identifying relationships between flood conditioning factors and their distribution. ML models such as ANN (Jahangir et al. 2019), random forest (Wang et al. 2015), K-nearest neighbor (Araghinejad et al. 2011), and x-gradient boost (Venkatesan and Mahindrakar 2019) have been widely used in flood susceptibility modeling and represent the models used in this study.

RF is an ensemble learning technique for classification and regression tasks. The original algorithm was created by Ho (1995) and later extended by Breiman (2001). As a parallel learning method, it operates on several decision trees trained randomly on different subsets. Consider Y the predicted value of a random forest model. Each individual tree predicts the value of Yi and the average value of the predicted values is the final value of Y. Y is calculated as follows:

$$\mathrm{Y} = \frac{1}{N}\sum_{n=1}^{N} \hat{f}_n(x)$$

where N is the total number of trees in the forest model and (f_n)ˆ(n) the prediction of the unknown value y of the tree n ($n = 1, 2\ldots N$). The number of trees is dependent on the task at hand (Venkatesan and Mahindrakar 2019).

RF algorithms manage to pick up highly complex and nonlinear relationships that exist between input and output variables. Moreover, overfitting decision trees to their training sets is corrected through this method.

XGB is an ensemble machine learning approach that is very fast, efficient, and scalable. It was developed by Friedman (2001). The prediction model is made up of several weak prediction models, usually decision trees. The output can be an integer in the case of classification problems or a real number when dealing with regression. The boosting algorithms are generalized by allowing the optimization of an arbitrary differentiable loss function. For instance, let K be the number of trees, the model can be defined as follows:

$$\sum_{k=1}^{K} f_k$$

where f_k is the prediction of the decision tree k ($k = 1, 2\ldots$ k) and the final model is an ensemble of decision trees. The final prediction can be defined as:

$$\hat{y}_i = \sum_{k=1}^{K} f_k(x_i)$$

where x_i is the feature vector of the i-th data point.

The loss function can be optimized using a metric—RMSE in the case of a regression. Regularization is used as a means of reducing the complexity of the model, thus preventing it from being overfitted and is defined as follows:

$$\Omega = \gamma T + \frac{1}{2}\lambda \sum_{j=1}^{T} {w_j}^2$$

where T is the number of leaves and wj^2 is the j-th leaf score. The objective of the model is the sum of the loss function and the regularization.

$$Obj = L + \Omega$$

where L is the differentiable convex loss function that measures the difference between the prediction $\hat{y}_i$ and the target y_i.

Finally, a gradient descent method is used to iteratively optimize the objective$Obj(y, \hat{y})$. It is determined as follows:

$$\partial \hat{y} Obj(y, \hat{y})$$

KNN is a supervised, non-parametric ML algorithm applicable to classification and regression problems. It takes as input the K-nearest learning examples, although the output depends on the classification or regression task. In the case of regression, the output is the average value of the K-nearest neighbors. On the other hand, the dominant class among the K-nearest neighbors (where k is an integer to be chosen) represents the output for classification problems. The three distance functions that KNN uses for both types of problems are:

Euclidean distance:

$$d(x_i, y_i) = \sqrt{\sum_{i=1}^{n} (x_i - y_i)^2}$$

Manhattan distance:

$$Manh.d(x_i, y_i) = \mid x_i - y_i \mid$$

Minkowski distance:

$$\text{Min}.d(x_i, y_i) = \left(\sum_{i=1}^{m} |x_i - y_i|^r \right)^{1/r}$$

where $X = (x\_1, x\_2, x\_3, \ldots, xn)$ and $Y = (y\_1, y\_2, y\_3, \ldots, yn)$ are two points in the feature space and n its dimensionality. The Euclidean distance is the most used of these three functions. By normalizing the training data, the accuracy of the KNN model can be greatly improved, since for classification the algorithm is distance based.

ANN was originally designed to emulate biological workings of neural networks in the animal brain. It was launched in 1962 by Frank Rosenblatt and refined most notably for its effectiveness in 1986 by Rumelhart and McClelland with the innovative perceptron model. ANN consists of a set of nodes called artificial neurons that are interconnected in a manner that allows them to transfer a signal, similarly to the biological neural network. When a signal (a real value) is received by a neuron, it is processed and sent to the neurons connected to it. Within each node and connection, there is a weight denoting the strength of the signal at a specific connection. During the learning process, this weight is adjusted to ensure that the cost function, defined as half the square difference between the actual and predicted values, is minimized. Upon each iteration, to adjust the weights, the cost function is fed back to the entire network. This process keeps going until the lowest cost function is reached. Then, the neurons are grouped into layers. A perceptron is a single-layer neural network. The performance of an artificial neural network can be improved, with the accuracy being enhanced by adding hidden layers between the input layer and the output layer.

The uniqueness of ANN lies in its ability to extract complex patterns from complex and ambiguous data. Indeed, these tasks would be impossible to achieve unaided or with existing computer approaches (Jahangir et al. 2019).

The Caret package (Kuhn 2014) was employed as a wrapper for the KNN, ANN, RF, and XGB implementations in R. The models were trained in parallel on 16 cores using the doParallel R package (Weston 2014).

Cross-validation and feature selection

The discrepancy between a model's performance estimated by a random test subset and the performance estimated by leave-one-out cross-validation (LOOCV) highlights overfitting due to inappropriate predictor variables (Meyer et al. 2016). It is critical to select robust variables to train a model

capable of successfully making predictions beyond the potential flood point sites. The feature selection methodology provides an efficient and intuitive approach to evaluating multiple models, resulting in the most significant variables (Guyon and Elisseeff 2003; Kuhn and Johnson 2013). Forward feature selection together with LOOCV was adopted to filter out variables that cause overfitting.

The best model was selected after training all models with all possible combinations of bivariate predictors. Model improvement was verified for every additional predictor using LOOCV. When none of the remaining variables reduced the root mean square error (RMSE) of the LOOCV to within a standard deviation of the most optimized model, the increase in the number of variables was discontinued (Meyer et al. 2016).

The CAST package for R was used as a wrapper for forward feature selection (Meyer et al. 2020). In this study, all four models were implemented both with and without variable selection.

Dealing with categorical variables

A lot of machine learning algorithms lack the ability to work directly on label data and require having all input variables be numeric, which is usually a major limitation for their successful implementation. Accordingly, the categorical data must be converted to a numeric form. The initial step is to perform integer coding, which involves assigning an integer value to each unique category value. This may suffice for some variables. Indeed, integers share a natural ordinal relationship between them, and ML algorithms are capable of learning and leveraging this behavior. In the case of categorical variables, without such an ordinal relationship, encoding in integers is not adequate. The use of this coding and the assumption of a natural order between categories in the model may result in unexpected results or performance problems. Thus, one-hot coding can be implemented for the representation of integers. Here, the integer-encoded variable is discarded, with a new binary variable being inserted for each individual integer value.

Transforming categorical variables can influence accuracy and model results. In this study, both the one-hot encoding approach and an approach without encoding were adopted for all four models in this study.

Models performance assessment

Since the purpose of the study is to apply the results in practice for predicting floods in the Souss watershed, it is essential to evaluate the performance and accuracy of the model before using it. Thus, the 174 data points—87 flooded and 87 non-flooded—were split into two parts using a random spatial partition method: 70% (122 points) as a training set and the remaining 30% (52 points) as a validation set. The training set and the validation set were used to train the model and evaluate the model performance, respectively. Training was performed by capturing the relationships between factors and flooding, and the resulting model was applied to the entire watershed.

The relative operating characteristic (ROC) curve was used as a means of measuring model performance. It characterizes the predictive accuracy of the model, describing the accuracy with which is it able to predict the occurrence of events (Mason and Graham 2002). Thus, high values imply better accuracy (Yesilnacar 2005; Al-Abadi and Al-Najar 2020). There are five area under the curve (AUC) classes: poor (0.5–0.6), medium (0.6–0.7), good (0.7–0.8), very good (0.8–0.9), and excellent (0.9–1).

Results

In this study, four models were developed for each of KNN, ANN, RF, XGB algorithms. One-hot encoding was used for the first model to transform categorical variables—aspect, flow direction, geology, land use, and soil type—while no transformation was performed for the second model. These categorical variables were retained as factors. A single model from the aforementioned models was created. It took the selected variables from the 13 available as inputs using a forward feature selection algorithm in the CAST package of R and another model whose inputs were simply the 13 variables. For instance, the models created for the random forest algorithm were RF without one-hot transformation without variable selection (RF), RF without one-hot transformation with variable selection (RF_SE), RF with one-hot transformation without variable selection (RF_TR), and RF with one-hot transformation with variable selection (RF_TR_SE).

Variable selection and variable importance

Through forward feature selection, unselected variables were identified as either leading to overfitting due to spatial autocorrelation or inappropriate for prediction. The variables selected for each model are presented in Table 1. In the forward feature selection, the number of predictor variables was reduced to only distance to rivers and soil type for the RF_SE model and DEM, drainage density, and NE aspect for the RF_TR_SE model. DEM, distance to rivers, and precipitation were selected for the XGB_SE model while DEM, distance to rivers, and drainage density for the XGB_SE_TR model. For the KNN models, the number of predictor variables was restricted to only DEM, distance to rivers, and drainage density for both the KNN_SE and KNN_SE_TR models. DEM and distance to river were the selected predictors for the KNN_SE model, while the northeast aspect

Table 1 Selected variables for the models

Models		Selected variables
KNN	KNN_SE	DEM, distance to rivers, and drainage density
	KNN_TR_SE	DEM, distance to rivers, and drainage density
ANN	ANN_SE	DEM and distance to rivers
	ANN_TR_SE	DEM, distance to rivers, and North aspect
RF	RF_SE	Distance to rivers and soil type
	RF_TR_SE	DEM, drainage density, and North-East aspect
XGB	XGB_SE	DEM, rainfall, and distance to rivers
	XGB_TR_SE	DEM, drainage density, and distance to rivers

was added for the KNN_SE_TR model. The results of the forward feature selection indicate that DEM, distance to rivers, drainage density, and rainfall are the most relevant predisposing factors in predicting flood susceptibility in the Souss watershed.

Variable importance scores for models that used all predictor variables revealed the significance of DEM, distance to rivers, and rainfall in predicting areas prone to flooding (Fig. 4). The most important variables for the RF models were DEM (100%), distance to rivers (57%), and precipitation (47%). Regarding the KNN model, the most important variables were rainfall (100%), DEM (99%), and distance to rivers (85%) while the most important variables for the ANN model were rainfall (100%), soil type (87%), and distance to rivers (86%). For the XGB models, rainfall (91%), soil type (46%), and distance to rivers (15%) were the most important. The relative importance of each variable is represented as a percentage.

Model evaluation and comparison

Evaluating the predictions of the models was based on the AUC value of the ROC curve. The ROC curves and AUC are presented in Table 2 and Figs. 5 and 6. The boxplot in Fig. 5 presents five sample statistics: minimum, lower quartile, median, upper quartile, and maximum. Of the RF models, the RF_SE_TR performed best as evidenced by the highest accuracy value (98.1%). Among the XGB models, the XGB_SE was the best performing, with an accuracy of 97.2%. KNN_SE and KNN_SE_TR were the best performing KNN models, with an identical accuracy

Table 2 Models' performance shown by the AUC score

Models		AUC (%)
KNN	KNN	94.6
	KNN_SE	98.6
	KNN_TR	95.1
	KNN_TR_SE	98.6
ANN	ANN	93.3
	ANN_SE	95.4
	ANN_TR	95.9
	ANN_TR_SE	95.4
RF	RF	96.7
	RF_SE	93.0
	RF_TR	96.7
	RF_TR_SE	98.1
XGB	XGB	95.9
	XGB_SE	97.2
	XGB_TR	94.1
	XGB_TR_SE	94.4

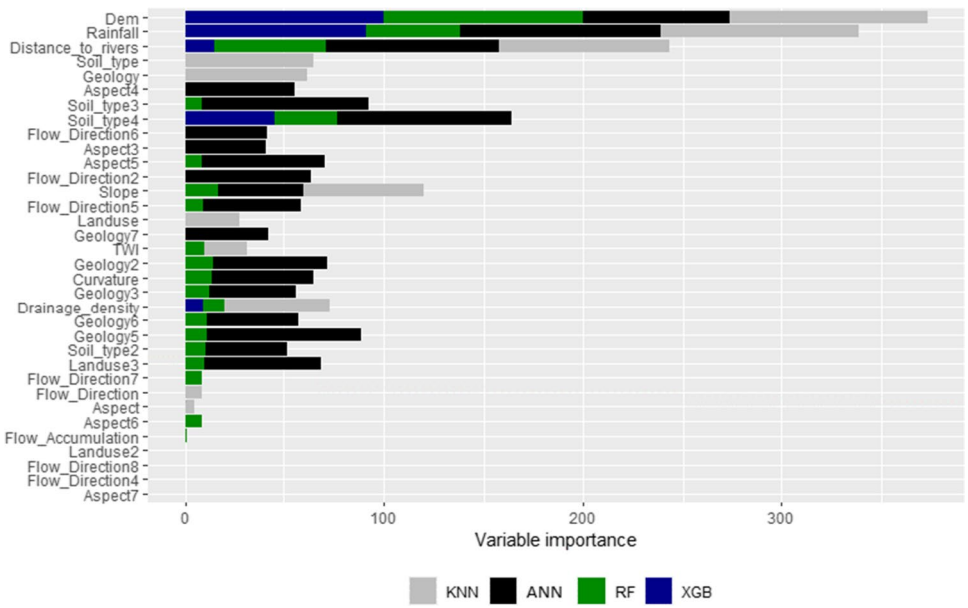

Fig. 4 Variable importance of the machine learning models

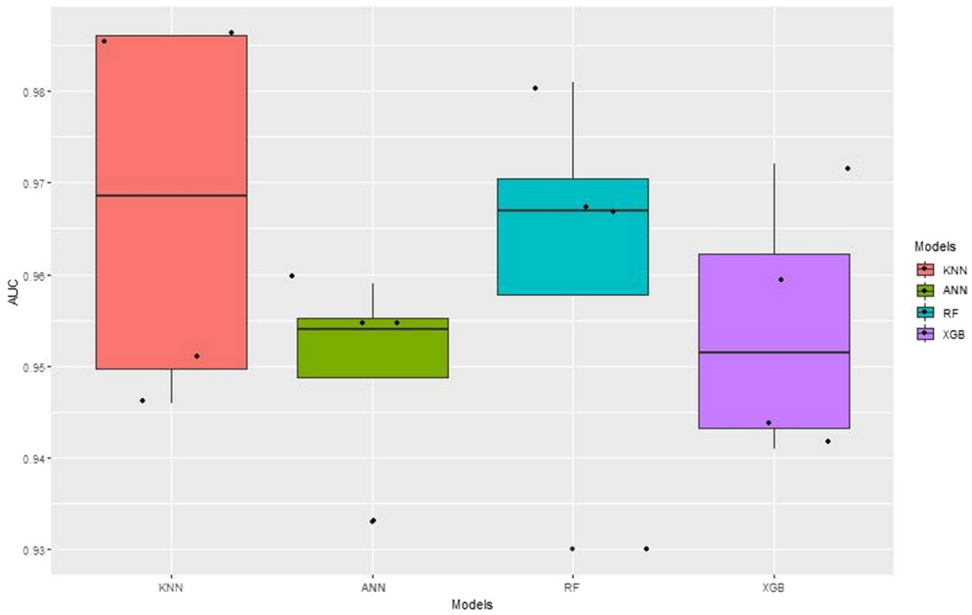

Fig. 5 Representation of the AUC of the model

of 98.6%. ANN_TR was the best performing ANN model with an accuracy of 95.9%.

Altogether, all models of the four algorithms scored an AUC above 80% for the test data (prediction rate), indicating that they all performed strongly. The most accurate models were KNN_SE and KNN_SE_TR, which produced the highest area under the curve (98.6%). The ranking of the ML algorithms, taking into account only the most efficient model of each algorithm is as follows: KNN (98.6%), RF (98.1%), XGB (97.2%), ANN (95.9%).

The results of the flood/non-flood point prediction for RF indicated over 94% of the flood points being placed in high to very high flood susceptibility classes, while less than 5% were placed in very low to low flood susceptibility classes (Table 3). For points assumed not to be floodable, 95% were assigned to very low to low flood susceptibility classes, while 0 and 1.45% were assigned to high to very high flood susceptibility classes, respectively (Table 3).

Flood susceptibility mapping

Flood susceptibility maps were developed for the sixteen models developed in this study (Fig. 7). Overall, they revealed the lower part of the Souss watershed to be highly vulnerable to flooding, while the upstream areas of the watershed were less vulnerable.

A study of the relationship between the probability of flood occurrence and the most relevant predictors was conducted based on forward feature selection and the importance of variables (Fig. 8, Table 4). Figure 8 presents the correlation between these two components for one thousand (1000) randomly sampled points using the susceptibility map for KNN_SE model since it proved to be the most accurate model. Table 4 presents the average probability of flood occurrence by predictor classes. The results suggested the probability of flood occurrence decreasing with increasing elevation (Fig. 8, Table 4).

The areas most susceptible to flooding were the low-lying areas, while areas of high elevation were less vulnerable. The same was true for distance to rivers and rainfall. As both distance to rivers and rainfall increased, vulnerability to flooding decreased in the Souss watershed. By contrast, the probability of flooding increased with increasing drainage density.

Models results comparison

The ML models adopted in this study performed reasonably well. Indeed, they had AUC values greater than 80%. Nevertheless, differences in model accuracy and overall performance remain, as was the case in this study. As such, it is imperative to compare model results to identify points of agreement and disagreement. Areas where the same classes of flood susceptibility were predicted were characterized by good models agreement. Conversely, the models disagreed where different classes of flood susceptibility were predicted. The uncertainty of the results is often low where all models agree and high where they disagree. The susceptibility maps were overlaid to make spatial comparisons of the model results. The four models of each model type (KNN, ANN, RF, XGB) were overlaid to compare their results. In addition, the sixteen models were overlaid to identify areas of agreement and disagreement.

The susceptibility maps were classified into five groups including very low (0–0.2), low (0.2–0.4), moderate (0.4–0.6), high (0.6–0.8), and very high (0.8–1) based on

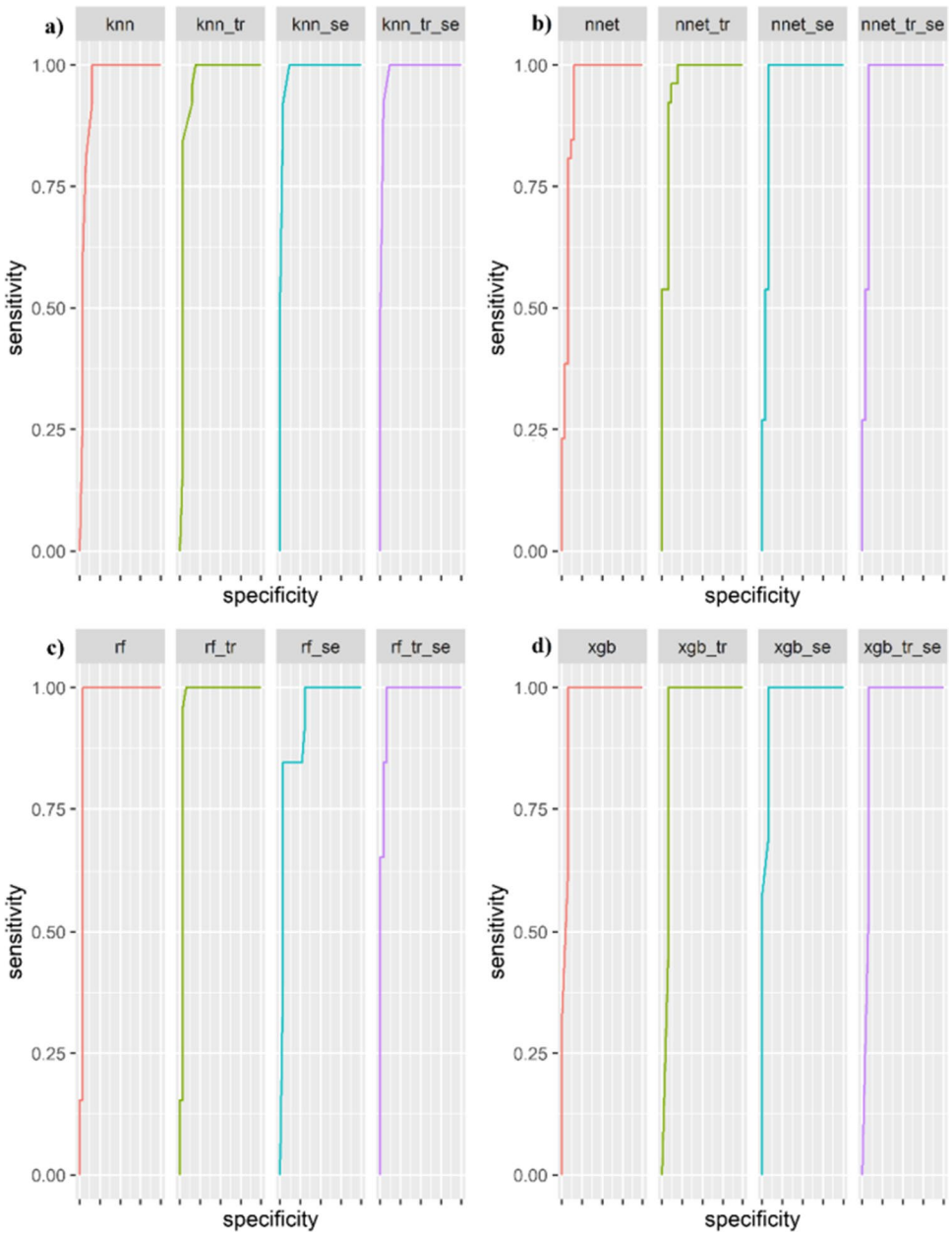

Fig. 6 Representation of the accuracy of the susceptibility model on testing data: **a** KNN, **b** ANN, **c** RF, and **d** XGB

Table 3 Prediction results for flood/non-flood points for RF model

	Flood/non-flood points per susceptibility class (%)					Total (%)
	Very low	Low	Moderate	High	Very high	
Flood points	1.15	3.45	1.15	1.15	93.10	100
Non-flood points	85.52	9.24	3.79	1.45	0.00	100

the probability of flood risk prior to comparing the model results (Fig. 9). The very low and very high susceptibility classes accounted for 23.68% and 57.01% of the watershed area, respectively. On the other hand, the low, moderate, and high susceptibility classes constituted 7.40%, 5.54%, and 6.37% of the watershed area, respectively. The probability of floods occurring was found to be greater than 80% for more than 57% of the watershed area, suggesting the Souss watershed as being highly vulnerable to flooding.

The maps presented in Fig. 10 show the areas of model agreement and disagreement regarding flood vulnerability. The four KNN models agreed in classifying 14.40%

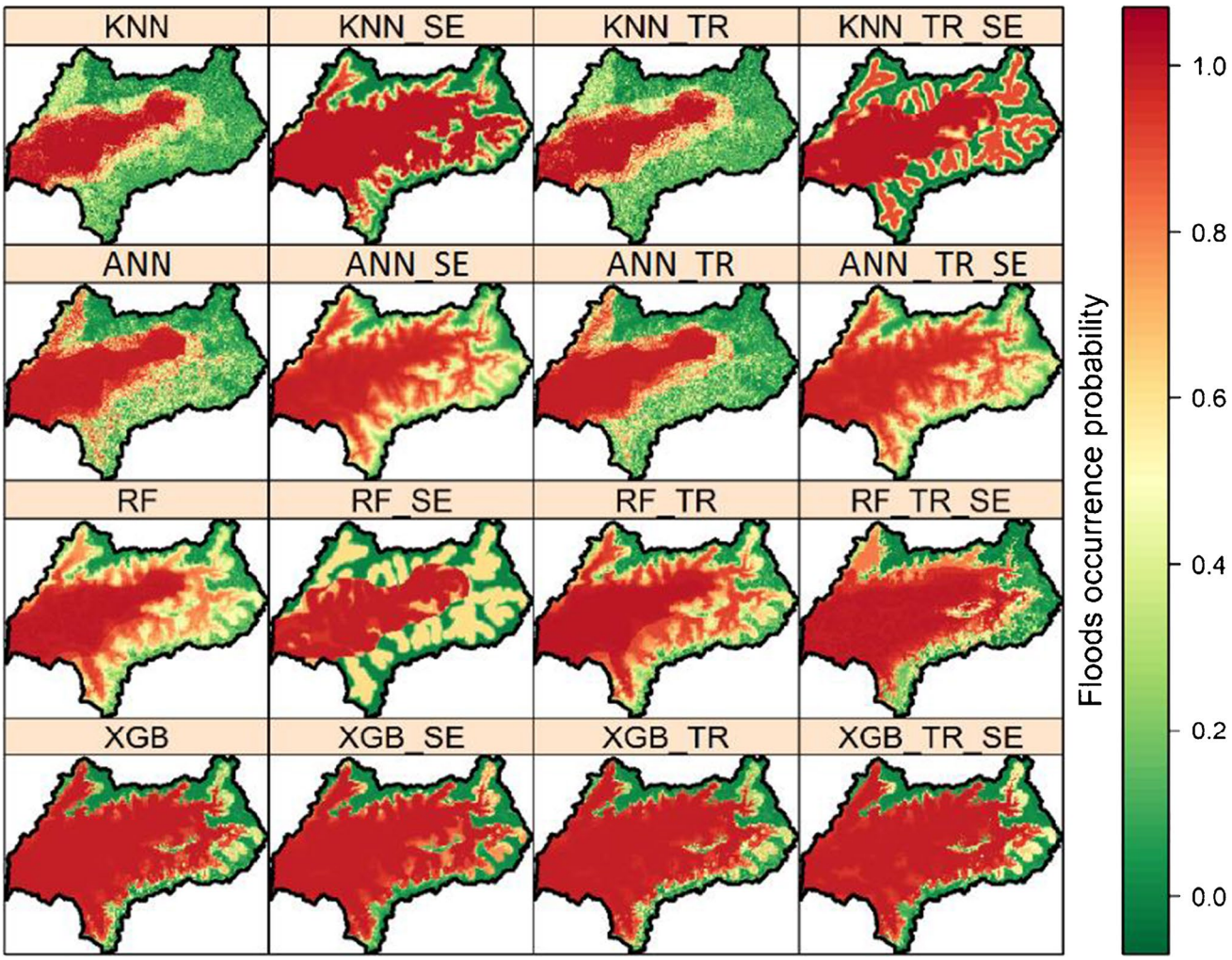

Fig. 7 Floods occurrence probability maps of all the models

and 26.13% of the watershed in the very low and very high susceptibility classes, respectively, while disagreeing in classifying 59.10% of the watershed area (Fig. 10 and Table 5). The ANN models agreed in classifying 10.74% and 34.84% of the watershed in the very low and very high susceptibility classes, respectively, while being in disagreement in classifying 52.73% of the watershed. On the other hand, the four RF models agreed in classifying 15.45% and 33.05% of the watershed in the very low and very high susceptibility classes, respectively, while disagreeing in classifying 52.42% of the watershed. The XGB models agreed in classifying 19.29% and 65.34% of the watershed in the very low and very high susceptibility classes, respectively, while disagreeing in classifying 14.58% of the watershed. The percentages of agreement were 40.9%, 47.27%, 47.58%, and 85.42% of the watershed area for the KNN, ANN, RF, and XGB models, respectively. This revealed a high similarity in the results of the XGB models compared to the KNN, ANN, and RF models. The XGB model emerged as less sensitive to variable selection and transformation of categorical variables in predicting flood susceptibility in the study.

The maps shown in Fig. 11 illustrate the areas of model agreement and disagreement with respect to susceptibility to flood risk. All models agreed in identifying 7.52% of the watershed area as having a very low risk of flooding and 25.3% being of very high risk (Fig. 11 and Table 5). By contrast, the models disagreed on the susceptibility to flooding of 67.15% of the watershed. These results can be applied with a high degree of certainty in the very low and very high susceptibility classes where all models agreed. On the other hand, areas where the models disagreed can be considered with some uncertainty as areas of moderate flood risk. Thus, these findings offer a useful tool for decision makers in implementing measures to mitigate flood risk in the Souss watershed.

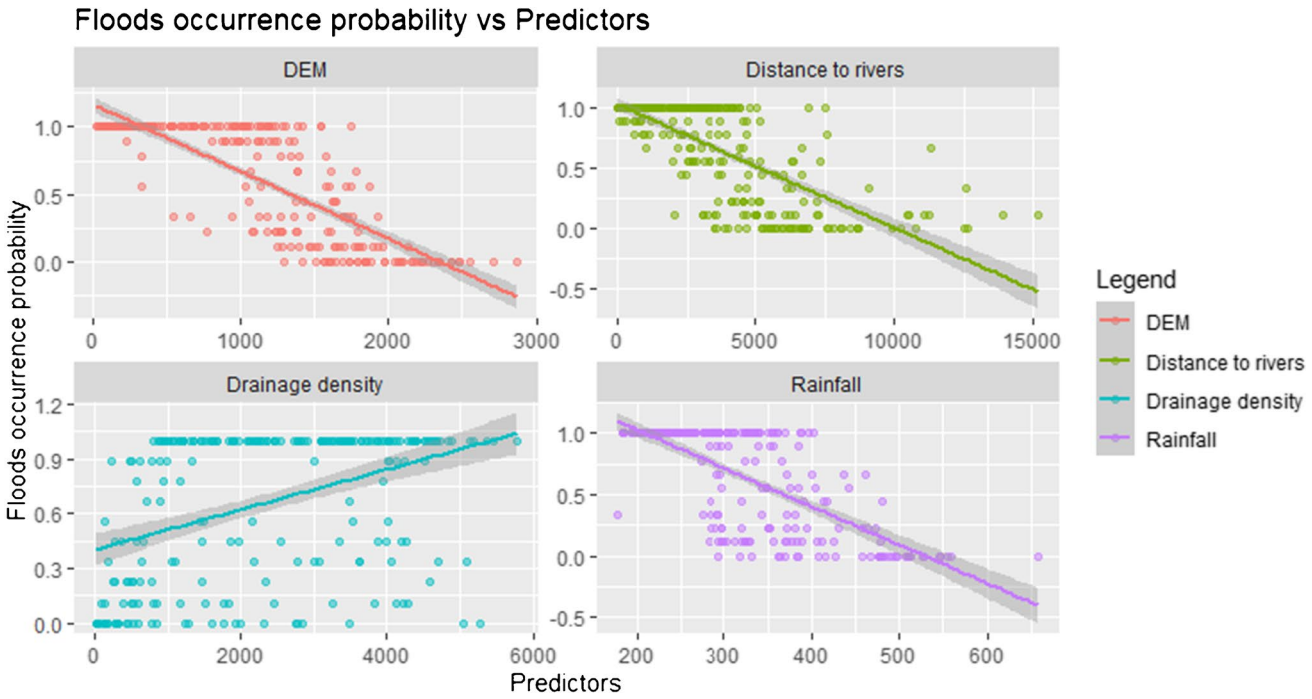

Fig. 8 Relationship between the flood's occurrence probability and the numerical predictors

Table 4 Relationship between the flood's occurrence probability and the selected predictors as relevant in the prediction for all the models

Models	Classes	Area (%)	Mean floods risk probability
DEM	0–500	25.41	0.99
	500–1000	18.37	0.86
	1000–1500	28.01	0.61
	1500–2000	20.48	0.25
	> 2000	7.73	0.07
Distance to rivers	0–1000	20.30	0.87
	1000–4000	41.60	0.76
	4000–6000	17.86	0.48
	6000–10000	16.48	0.30
	> 10000	3.75	0.22
Drainage density	< 1000	24.04	0.35
	1000–2000	18.19	0.65
	2000–3000	20.84	0.71
	3000–4000	20.72	0.74
	> 4000	16.21	0.83
Rainfall	< 200	4.01	0.99
	200–300	38.17	0.93
	300–400	39.05	0.53
	400–500	13.70	0.23
	> 500	5.07	0.06

Discussion

Dedicated flood susceptibility maps can be used by policymakers and risk managers to mitigate flooding, thereby reducing damages to infrastructure and harm to the affected population. Selecting the most effective and the best-performing ML algorithm can be challenging due to the complex nature of the data in flood susceptibility modeling (Mohammadi et al. 2018).

In this study, four ML algorithms including RF, XGB, KNN, and ANN were used. Their ranking from the most efficient to the least was KNN (98.6%), RF (98.1%), XGB (97.2%), and ANN (95.9%). Similarly, high accuracy models have been noted in the literature in studies involving the assessment of flood susceptibility. In studies performed in Iran, both Mirzaei et al. (2020) and Naghibi et al. (2019) identified RF to be the most effective model, with prediction accuracy values of 98.5% and 97.1%, respectively. Furthermore, Mirzaei et al. (2020) reported gradient boost to be equally effective, with an AUC of 98.0%. This result is consistent with our study. Correspondingly, Naghibi et al. (2019) highlighted the greater accuracy of the KNN model, with an AUC of 94.6%. Madhuri et al. (2021), comparing the performance of ML algorithms for flood susceptibility prediction, showed that XGB outperformed KNN with AUCs of 83% and 66% respectively, while in this study, KNN outperformed XGB. The ANN method was equally effective, although it had the lowest predictive accuracy of the

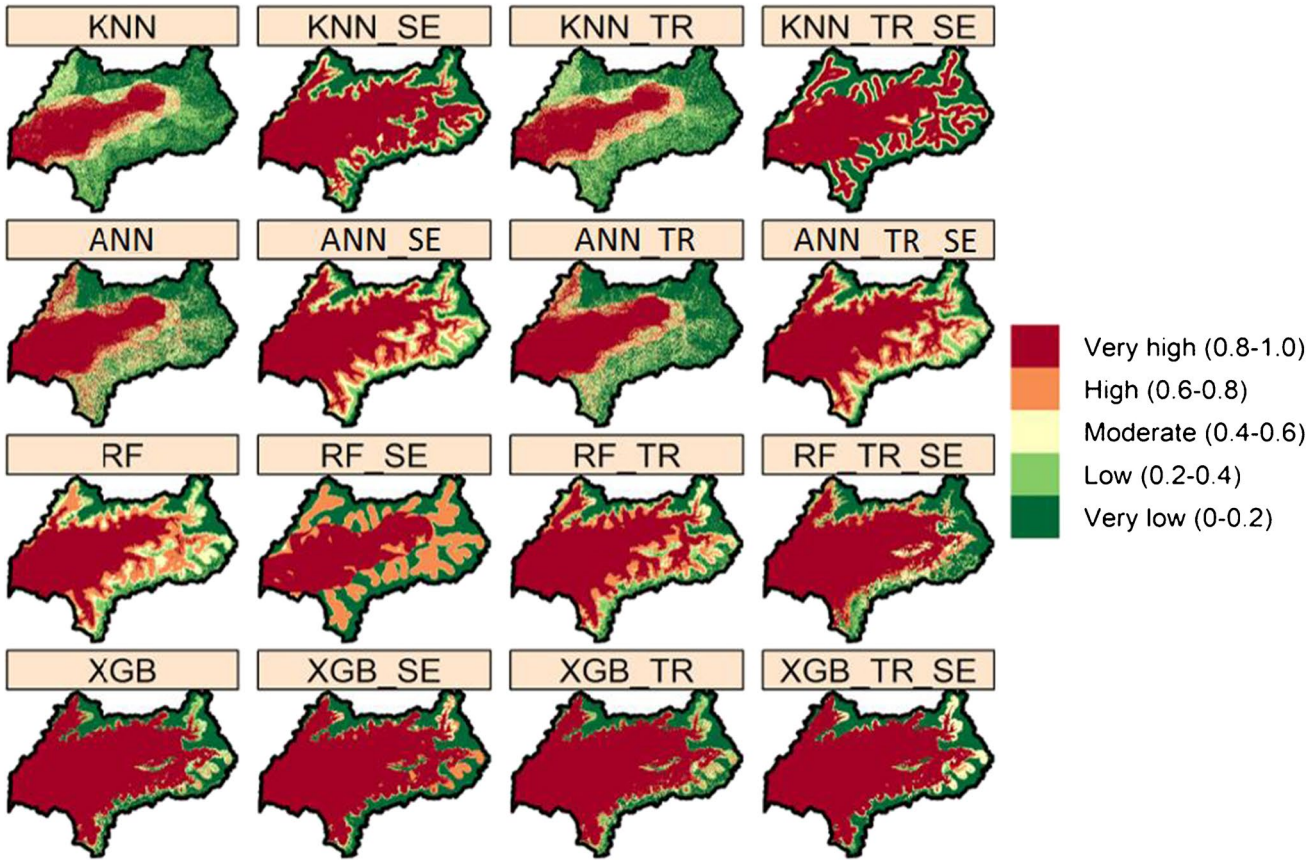

Fig. 9 Flood susceptibility maps classified in five classes for all the models

four approaches studied. Indeed, at 95.9%, it outperformed the same model in the work done Avand et al. (2021) who recorded an AUC value of 89.7%. As such, this study provides evidence that the selected models are realistically feasible due to their performance and ease of interpretation.

The choice of flood conditioning factors is paramount in flood susceptibility mapping. How many, and which factors should be chosen to best describe the physical characteristics determining the flood susceptibility of the study area, is the first contentious issue. For the purpose of this study, thirteen predisposing factors were chosen on the basis of other flood susceptibility studies (Kourgialas and Karatzas 2011; Elkhrachy 2015; Kazakis et al. 2015; Rahmati et al. 2016; Samanta et al. 2016; Khosravi et al. 2016; Haghizadeh et al. 2017; Zhao et al. 2018; Mahmoud and Gan 2018; Choubin et al. 2019). While some authors used only four factors (Rahmati et al. 2016; Samanta et al. 2016), others used six (Kourgialas and Karatzas 2011), ten (Haghizadeh et al. 2017; Khosravi et al. 2016), eleven (Choubin et al. 2019), or twelve conditioning factors (Zhao et al. 2018). However, there has been no clear consensus on which set of factors should be used for flood sensitivity analysis. Nevertheless, some analysts have suggested the using not fewer than factors to mitigate the potential of overpredicting flooding contributing factors (Mahmoud and Gan 2018). In this study, aspect, curvature, elevation, distance to rivers, drainage density, flow accumulation, flow direction, geology, land use, precipitation, slope, soil type, and TWI were selected. Elevation, rainfall, distance to rivers, and drainage density were identified as the most relevant and important predictors in predicting flood susceptibility areas in the Souss watershed based on the results of the feature selection and variable importance scores. These findings are in line with the study carried out on the Tajan watershed in Iran by Avand et al. (2021). Indeed, they identified similar flood conditioning factors as being the most pertinent.

Elevation is a driving factor in the occurrence of flooding, as water always flows from higher elevations to lower elevations. In fact, the probability of flooding increases with decreasing elevation. In the Souss watershed, it was found to be the most important factor in predicting areas of flood susceptibility. This is consistent with previous studies, which highlighted low probability of flooding in higher elevations and high likelihood of flooding in low-lying areas (Khosravi et al. 2019; Das 2019). Rainfall has been reported in the literature as an important conditioning factor in determining

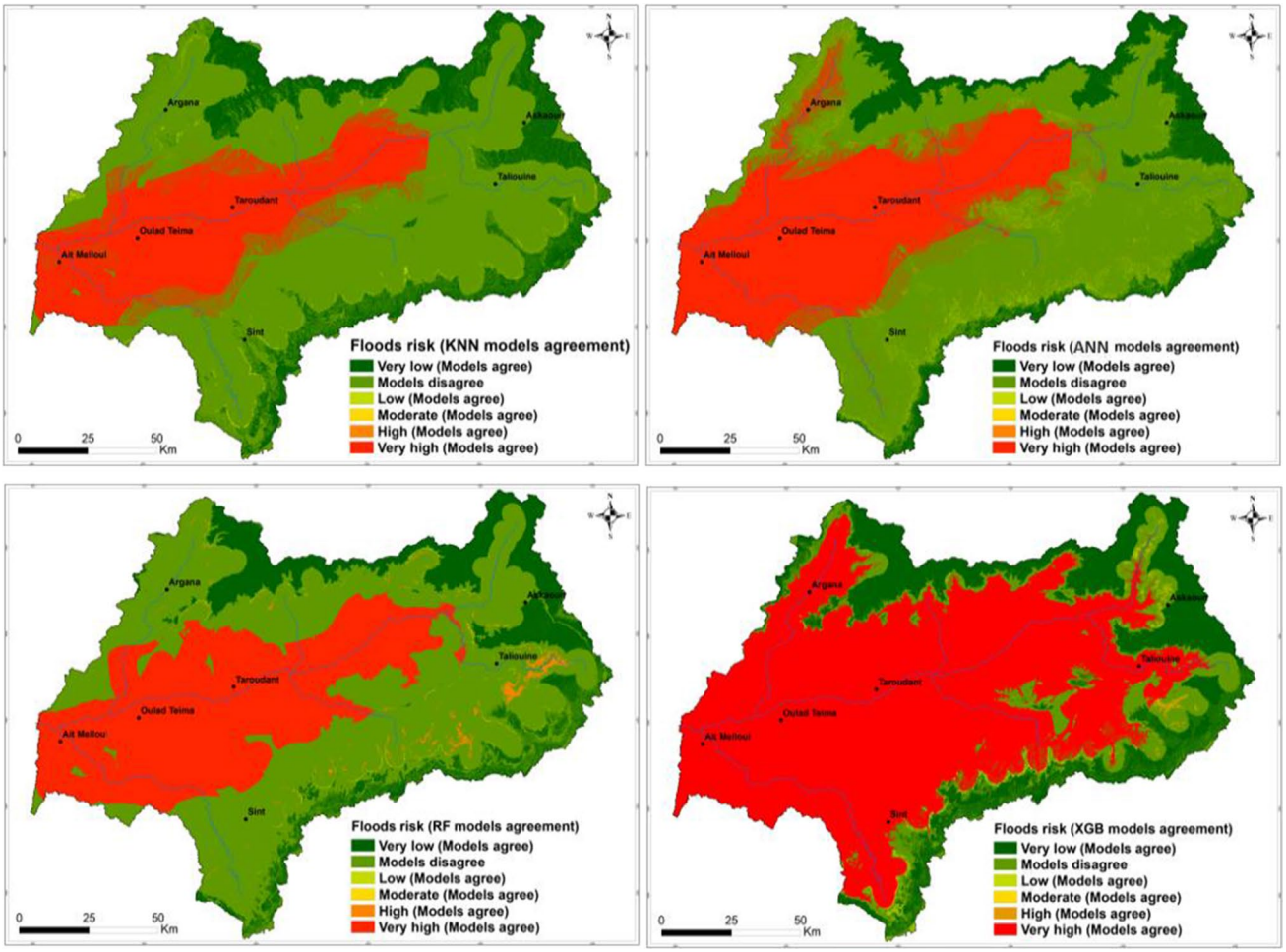

Fig. 10 Models' results comparison for each kind of model

the flood event. Generally, heavy rainfall increases the likelihood of flooding in susceptible areas (Todini et al. 2004). Conversely, the Souss watershed was characterized by a low probability of flood occurrence in areas with high rainfall and a high probability of flooding in areas with low rainfall. This can be attributed to the correlation between rainfall and altitude, which is the main conditioning factor in the study area, where rainfall increases with altitude.

In this study, distance to rivers stands out as one of the prominent factors in the determining the probability of flood events. This observation was also reported by Ahmadlou et al. (2018), Bui et al. (2018), and Shafizadeh-Moghadam et al. (2018). Water levels in rivers increase due to increased rainfall during flood events, causing water to overflow into areas closer to the shore (Tehrany et al. 2014). Thus, areas that lie adjacent to rivers and floodplains are at the greatest risk of flooding.

Drainage density is recognized as a significant contributor to flooding. Increased probability of flooding is strongly related to higher drainage density, as it indicates higher surface runoff (Das 2019; Paul et al. 2019). In this research, drainage density bears a direct link to flooding.

Modeling flooding is a challenging task with many associated uncertainties. ML algorithms are able to efficiently tackle these uncertainties with the help of reliable historical inventory maps. While the ML models discussed in this study are not new, they provide a valuable alternative for policy-makers in predicting natural hazards in the Moroccan territory. The methods explored in this study were shown to be highly accurate yet reasonably straightforward. Combined with the fact that they require significantly less time and resources than the more traditional physical and statistical methods, they represent a valuable resource for stakeholders involved in risk assessment. Indeed, they are a vital tool for flood prediction in the Souss watershed, where the application of the ML method has been minimal if not completely absent. Moreover, this approach is easily applicable not only to other regions of the country but also to neighboring countries in the Mediterranean region, with similar environments. This is due to the ease with which the adopted

Table 5 Models' agreement results

Models	Classes	Area (%)
All	Very low risk (all models agree)	7.52
	All models disagree	67.15
	Very high risk (all models agree)	25.33
KNN	Very low (models agree)	14.40
	Models disagree	59.10
	Low (models agree)	0.28
	Moderate (models agree)	0.06
	High (models agree)	0.03
	Very high (models agree)	26.13
ANN	Very low (models agree)	10.74
	Models disagree	52.73
	Low (models agree)	0.65
	Moderate (models agree)	0.43
	High (models agree)	0.61
	Very high (models agree)	34.84
RF	Very low (models agree)	14.45
	Models disagree	51.42
	Low (models agree)	0.11
	Moderate (models agree)	0.12
	High (models agree)	0.84
	Very high (models agree)	33.05
XGB	Very low (models agree)	19.29
	Models disagree	14.58
	Low (models agree)	0.24
	Moderate (models agree)	0.33
	High (models agree)	0.22
	Very high (models agree)	65.34

ML approaches deal with the complexity of hydrological processes coupled with the availability of parameters used for the models.

Conclusion

Floods are one of the most destructive natural hazards occurring in the world. In this study, 16 models based on ML algorithms including KNN, ANN, RF, and XGB were compared for their performance in mapping flood susceptibility in the Souss watershed. Using these models, the relationships between flooding and conditioning factors such as aspect, curvature, DEM, distance to rivers, drainage density, flow accumulation, flow direction, geology, land use, precipitation, slope, soil type, and TWI were adequately characterized.

Upon analyzing the model prediction results, the most prominent factors in predicting flood risk were identified. On the whole, DEM, distance to rivers, and precipitation were determined to be the most relevant factors in mapping flood susceptibility based on the fact that they were selected at least once by the selection algorithm. Moreover, they provided a high percentage of significance for the development of certain models.

The ROC curve was used to determine the performance of the models. For each algorithm, the AUC of the best model was 98.1%, 97.2%, 98.6%, and 95.9% for RF, XGB, KNN, and ANN, respectively. Finally, the results of this study are proof that flood susceptibility mapping projects in Morocco have the potential to be accomplished using ML models. Indeed, susceptibility maps could serve as a useful tool for

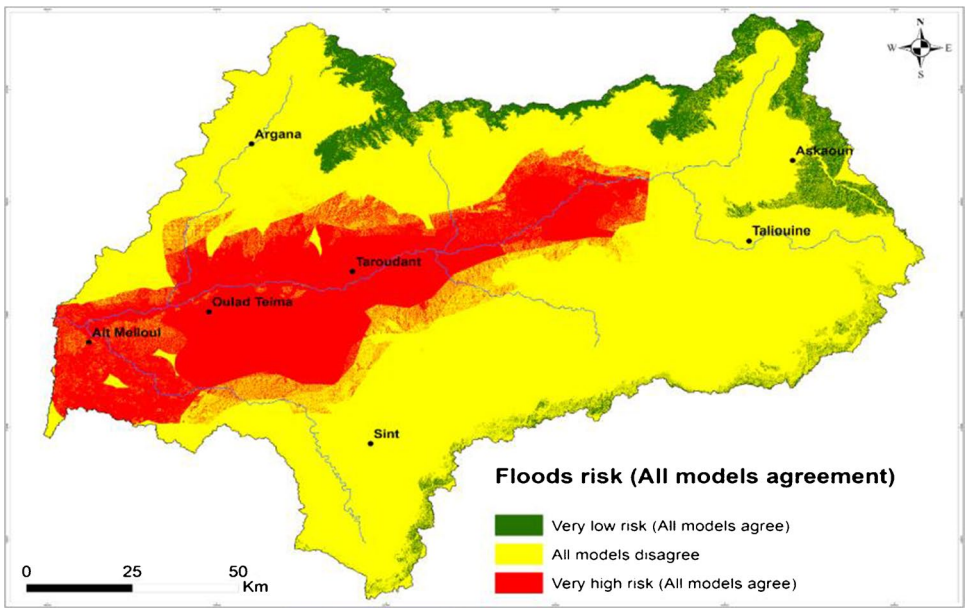

Fig. 11 Models' results comparison for all models

flood management and for mitigating the damage caused by these events in vulnerable areas.

Acknowledgments This study was carried out within the framework of the Initiative "Environmental and Socio-Economic Vulnerability and Adaptation Potential to Climate Change in the Rural Commune of El Faid," implemented by the Moroccan Regional Science Association, Rabat, and supported by Ouranos, Canada, through a partial funding from the Green Fund under the Government of Quebec's 2013–2020 Climate Change Action Plan.

Declaration

Competing interests The authors declare that they have no competing interests.

References

Abbot J, Marohasy J (2017) The application of machine learning for evaluating anthropogenic versus natural climate change. Geo Res J 14:36–46

Ahmadlou M, Karimi M, Alizadeh S, Shirzadi A, Parvinnejhad D, Shahabi H, Panahi M (2018) Susceptibility assessment using integration of adaptive network-based fuzzy inference system (ANFIS) and biogeography-based optimization (BBO) and bat algorithms (BA). Geocarto Int. 34:1–21

Al-Abadi AM, Al-Najar NA (2020) Comparative assessment of bivariate, multivariate and machine learning models for mapping flood proneness. Nat Hazards 100:461–491

Al-Juaidi AE, Nassar AM, Al-Juaidi OE (2018) Evaluation of flood susceptibility mapping using logistic regression and GIS conditioning factors. Arab J Geosci 11:765

Araghinejad S, Azmi M, Kholghi M (2011) Application of artificial neural network ensembles in probabilistic hydrological forecasting. J Hydrol 407:94–104

Avand M, Moradi HR, Ramazanzadeh LM (2021) Spatial prediction of future flood risk: an approach to the effects of climate change. Geosciences 11:25

Ayalew L, Yamagishi H (2005) The application of GIS-based logistic regression for landslide susceptibility mapping in the Kakuda-Yahiko Mountains. Geomorphology 65:15–31

Breiman L (2001) Random Forests. Mach Learn 45:5–32

Buchhorn M, Smets B, Bertels L, De Roo B, Lesiv M, Tsendbazar NE, Herold M, Fritz S (2018) Copernicus Global Land Service: land cover 100m: collection 3: epoch 2018: Globe 2020

Bui D, Panahi M, Shahabi H, Singh V, Shirzadi A, Chapi K, Khosravi K, Chen W, Panahi S, Li S, Ahmad B (2018) Novel hybrid evolutionary algorithms for spatial prediction of floods. Sci Rep 8:15364

Campolo M, Soldati A, Andreussi P (2003) Artificial neural network approach to flood. Hydrolog Sci J 48:381–398

Cao C, Xu P, Wang Y, Chen J, Zheng L, Niu C (2016) Flash Flood hazard susceptibility mapping using frequency ratio and statistical index methods in coalmine subsidence areas. Sustainability 8:948

Carrara A, Guzzetti F, Cardinali M (1999) Use of GIS technology in the prediction and monitoring of landslide hazard. Nat Hazards 20:117–135

Chapi K, Singh VP, Shirzadi A, Shahabi H, Bui DT, Pham BT, Khosravi K (2017) A novel hybrid artificial intelligence approach for flood susceptibility assessment. Environ Modell Softw 95:229–245

Choubin B, Moradi E, Golshan M, Adamowski J, Sajedi-Hosseini F, Mosavi A (2019) An ensemble prediction of flood susceptibility using multivariate discriminant analysis, classification and regression trees, and support vector machines. Sci Total Environ 651:2087–2096

Das S (2019) Geospatial mapping of flood susceptibility and hydrogeomorphic response to the floods in Ulhas basin, India. Remote Sens Appl Soc Environ 14:60–74

Diakakis M, Deligiannakis G, Pallikarakis A, Skordoulis M (2016) Factors controlling the spatial distribution of flash flooding in the complex environment of a metropolitan urban area. The case of Athens 2013 flash flood event. Int J Disast Risk Re 18:171–180

Doocy S, Daniels A, Packer C, Dick A, Kirsch TD (2013) The human impact of earthquakes: a historical review of events 1980-2009 and systematic literature review. PLoS Curr 16:5

Elkhrachy I (2015) Flash flood hazard mapping using satellite images and GIS tools: a case study of Najran City, Kingdom of Saudi Arabia (KSA). Egypt. J Remote Sens Space Sci 18:261–278

Elmouden A, Alahiane N, El Faskaoui M, El Morjani ZEA (2016) Dams Siltation and soil erosion in the souss–massa river basin. Handbook Environ Chem 53:95–120

El Morjani ZEA, Seif Ennasr M, Elmouden A, Idbraim S, Bouaakaz B, Saad A (2016) Flood hazard mapping and modeling using GIS applied to the souss river watershed. Handbook Environ Chem 57–93

FAO/IIASA/ISRIC/ISSCAS/JRC (2012) Harmonized World Soil Database (version 1.2). FAO, Rome, Italy and IIASA, Laxenburg, Austria

Friedman J (2001) Greedy boosting approximation: a gradient boosting machine. Ann Stat 29:1189–1232

Guyon I, Elisseeff A (2003) An introduction to variable and feature selection. J Mach Learn Res 3:1157–1182

Haghizadeh A, Siahkamari S, Hamzeh Haghiabi A, Rahmati O (2017) Forecasting flood-prone areas using Shannon's entropy model. J Earth Syst Sci 126:39

Ho TK (1995) Random Decision Tree (PDF). Proceedings of the 3rd International Conference on Document Analysis and Recognition, Montreal, QC, 14–16 August 1995. pp. 278–282

Hosseiny H, Nazari F, Smith V, Nataraj C (2020) A framework for modeling flood depth using a hybrid of hydraulics and machine learning. Sci Rep 10:8222

Hssaisoune M, Boutaleb S, Mohammed B, Bouaakkaz B, Bouchaou L (2016) Physical geography, geology, and water resource availability of the Souss-Massa River Basin. Handbook Environ Chem 53:27–56

Jahangir MH, Mousavi Reineh SM, Abolghasemi M (2019) Spatial predication of flood zonation mapping in Kan River Basin, Iran, using artificial neural network algorithm. Weather Clim Extrem 25:100215

Jayakrishnan R, Srinivasan R, Santhi C, Arnold J (2005) Advances in the application of the SWAT model for water resources management. Hydrol Process 19:749–762

Jutras S, Rousseau A, Clerc C (2009) Implementation of a Peatland-specific water budget algorithm in HYDROTEL. Can Water Resour J 34(4):349–364

Kazakis N, Kougias I, Patsialis T (2015) Assessment of flood hazard areas at a regional scale using an index-based approach and analytical hierarchy process: application in Rhodope-Evros region. Greece Sci Total Environ 538:555–563

Khosravi K, Pham BT, Chapi K, Shirzadi A, Shahabi H, Revhaug I (2018) A comparative assessment of decision trees algorithms for flash flood susceptibility modeling at Haraz watershed, northern Iran. Sci Total Environ 627:744–755

Khosravi K, Nohani E, Maroufinia E, Pourghasemi HR (2016) A GIS-based flood susceptibility assessment and its mapping in Iran: a comparison between frequency ratio and weights-of-evidence bivariate statistical models with multi-criteria decision-making technique. Nat Hazards 83:947–987

Khosravi K, Melesse A, Shahabi H, Shirzadi A, Chapi K, Hong H (2019) Flood susceptibility mapping at Ningdu catchment, China using bivariate and data mining techniques. Extrem Hydrol Clim Variabil 419–434

Kim S, Matsumi Y, Pan S, Mase H (2016) A real-time forecast model using artificial neural network for after- runner storm surges on the Tottori coast, Japan. Ocean Eng 122:44–53

Kourgialas NN, Karatzas GP (2011) Flood management and a GIS modelling method to assess flood-hazard areas-A case study. Hydrol Sci J 56:212–225

Kron W (2005) Flood Risk = Hazard • Values • Vulnerability. Water Int 30(1):58–68

Kron W (2002) Flood risk = hazard × exposure × vulnerability. In: Wu M et al (eds) Flood Defence. Science Press, New York, pp 82–97

Kuhn M (2014) Caret: classification and regression training, R package version 6.0-29. CRAN, Wien 37

Kuhn M, Johnson K (2013) Applied predictive modeling, 1st edn. Springer, New York

Lee S, Kim JC, Jung HS, Lee MJ, Lee S (2017) Spatial prediction of flood susceptibility using random-forest and boosted-tree models in Seoul metropolitan city, Korea. Geomat Nat Haz Risk 8(2):1185–1203

Li-Hua F, Jia L (2010) The practical research on flood forecasting based on artificial neural networks. Expert Syst Appl 37:2974–2977

Liu R, Chen Y, Wu J (2016) Assessing spatial likelihood of flooding hazard using naïve Bayes and GIS: a case study in Bowen Basin, Australia. Stoch Env Res Risk A 3:1575–1590

Madhuri R, Sistla S, Srinivasa Raju K (2021) Application of machine learning algorithms for flood susceptibility assessment and risk management. J Water Climate Change 12(6):2608–2623

Mahmoud SH, Gan TY (2018) multi-criteria approach to develop flood susceptibility maps in arid regions of Middle East. J Clean Prod 196:216–229

Mason SJ, Graham NE (2002) Areas beneath the relative operating characteristics (ROC) and relative operating levels (ROL) curves: Statistical significance and interpretation. Q J Roy Meteor Soc 128:2145–2166

Mekanik F, Imteaz M, Gato-Trinidad S, Elmahdi A (2013) Multiple regression and Artificial Neural Network for long-term rainfall forecasting using large scale climate modes. J Hydrol 503:11–21

Meliho M, Khattabi A, Mhammdi N (2018) A GIS-based approach for gully erosion susceptibility modelling using bivariate statistics methods in the Ourika watershed. Morocco. Environ Earth Sci 77:18

Meyer H, Katurji M, Appelhans T, Müller M, Nauss T, Roudier P, Zawar-Reza P (2016) Mapping daily air temperature for antarctica based on MODIS LST. Remote Sens 8(9):732

Meyer H, Reudenbach C, Ludwig M, Nauss T, Pebesma E (2020) Package 'CAST'. CRAN, Wien, p 13

Mirzaei S, Vafakhah M, Pradhan B, Alavi SJ (2020) Flood susceptibility assessment using extreme gradient boosting (EGB), Iran. Earth Sci Infor 14:51–67

Mohammadi A, Shahabi H, Bin Ahmad B (2018) Integration of Insar technique, Google earth images, and extensive field survey for landslide inventory in a part of Cameron highlands, Pahang, Malaysia. Appl Ecol Environ Res 16:8075–8091

Mosavi A, Ozturk P, Chau K (2018) Flood prediction using machine learning models: literature review. Water 10(11):1536

Mosavi A, Rabczuk T, Varkonyi-Koczy AR (2017) Reviewing the novel machine learning tools for materials design. International Conference on Global Research and Education, 50-58

Naghibi SA, Vafakhah M, Hashemi H, Pradhan B, Alavi SJ (2019) Water resources management through flood spreading project suitability mapping using frequency ratio, k-nearest neighbours, and random forest algorithms. Nat Resour Res 29:1915–1933

Paul GC, Saha S, Hembram TK (2019) Application of the GIS-based probabilistic models for mapping the flood susceptibility in Bansloi sub-basin of Ganga-Bhagirathi river and their comparison. Remote Sens Earth Syst Sci 2:120–146

Tien Bui D, Khosravi K, Shahabi H, Daggupati P, Adamowski JF, Melesse MA, Lee S (2019) Flood spatial modeling in Northern Iran using remote sensing and GIS: a comparison between evidential belief functions and its ensemble with a multivariate logistic regression model. Remote Sens 11(13):1589

Todini F, De Filippis T, De Chiara G, Maracchi G, Martina M, Todini E (2004) Using a GIS approach to asses flood hazard at national scale. In Proceedings of the European Geosciences Union, 1st General Assembly, Nice, France, 25–30 April 2004

Opolot E (2013) Application of remote sensing and geographical information systems in flood management: a review. Res J Appl Sci Eng Technol 6(10):1884–1894

Pradhan B, Shafiee M, Pirasteh S (2010) Maximum flood prone area mapping using RADARSAT images and GIS: Kelantan River basin. Int J Geoinformatics 5:11

Pradhan B (2009) Flood susceptible mapping and risk area delineation using logistic regression, GIS and remote sensing. J Spat Hydrol 9:1–18

Rahmati O, Zeinivand H, Besharat M (2016) Flood hazard zoning in Yasooj region, Iran, using GIS and multi-criteria decision analysis. Geomat. Nat. Hazards Risk 7:1000–1017

Albano R, Sole A (2018) Geospatial methods and tools for natural risk management and communications. ISPRS Int J Geo-Inf 7:470

Samanta RK, Bhunia GS, Shit PK, Pourghasemi HR (2018) Flood susceptibility mapping using geospatial frequency ratio technique: a case study of Subarnarekha River Basin, India. Model Earth Syst Environ 4(1):395–408

Samanta S, Koloa C, Kumar Pal D, Palsamanta B (2016) Flood risk analysis in lower part of Markham River based on multi-criteria decision approach (MCDA). Hydrology 3:29

Seckin N, Cobaner M, Yurtal R, Haktanir T (2013) Comparison of artificial neural network methods with L-moments for estimating flood flow at ungauged sites: the case of East Mediterranean River Basin, Turkey. Water Resour Manage 27(7):2103–2124

Shafizadeh-Moghadam H, Valavi R, Shahabi H, Chapi K, Shirzadi A (2018) Novel forecasting approaches using combination of machine learning and statistical models for flood susceptibility mapping. J Environ Manage. 217:1–11

Shahab A, Monte A, Majid K (2011) Application of artificial neural network ensembles in probabilistic hydrological forecasting. J Hydrol 407:94–104

Sahana M, Patel PP (2019) A comparison of frequency ratio and fuzzy logic models for flood susceptibility assessment of the lower Kosi River Basin in India. Environ Earth Sci 78(10):289

Shu C, Burn DH (2004) Artificial neural network ensembles and their application in pooled flood frequency analysis. Water Resour Res 40:W09301

Srivastava OS, Denis D, Srivastava SK, Kumar M (2014) Morphometric analysis of a Semi Urban Watershed, trans Yamuna, draining at Allahabad using Cartosat (DEM) data and GIS. Int J Eng Sci 3:71–79

Tehrany MS, Pradhan B, Jebur MN (2014) Flood susceptibility mapping using a novel ensemble weights-of-evidence and support vector machine models in GIS. J Hydrol 512:332–343

Tehrany MS, Pradhan B, Mansor S, Ahmad N (2015) Flood susceptibility assessment using GIS-based support vector machine model with different kernel types. CATENA 125:91–101

Tehrany HM, Kumar L, Shabani F (2019) A novel GIS-based ensemble technique for flood susceptibility mapping using evidential belief function and support vector machine: Brisbane, Australia. Peer J 7:1–32

Tien Bui D, Shirzadi A, Chapi K, Shahabi H, Pradhan B, Pha B, Lee S (2019b) A Hybrid Computational Intelligence Approach to Groundwater Spring Potential Mapping. Water 11(10):2013

Tien Bui D, Pradhan B, Nampak H, Bui QT, Tran QA, Nguyen QP (2016) Hybrid artificial intelligence approach based on neural fuzzy inference model and metaheuristic optimization for flood susceptibility modeling in a high-frequency tropical cyclone area using GIS. J Hydrol 540:317–330

Townsend PA, Walsh SJ (1998) Modeling floodplain inundation using an integrated GIS with radar and optical remote sensing. Geomorphology 21(3-4):295–312

Venkatesan E, Mahindrakar AB (2019) Forecasting floods using extreme gradient boosting – A new approach. Int J Civ Eng 10:1336–1346

Wang Z, Lai C, Chen X, Yang B, Zhao S, Bai X (2015) Flood hazard risk assessment model based on random forest. J Hydrol 527:1130–1141

Weston S (2014) doParallel: Foreach Parallel Adaptor for the Parallel Package, R package version 1.0.8. CRAN, Wien

Xu ZX, Li JY (2002) Short-term inflow forecasting using an artificial neural network model. Hydrol Process 16:2423–2439

Yesilnacar EK (2005) Application of Neural Networks for Landslide Susceptibility Mapping in Turkey. In: Van Leeuwen JP, HJP T (eds) Recent Advances in Design & Decision Support Systems in Architecture and Urban Planning. Kluwer Academic Publishers, ISBN: 14020-2408-8, Dordrecht, pp 3–18

Zhao G, Pang B, Xu Z, Yue J, Tu T (2018) Mapping flood susceptibility in mountainous areas on a national scale in China. Sci Total Environ 615:1133–1142

Zkhiri W, Tramblay Y, Hanich L, Berjamy B (2016) Regional flood frequency analysis in the High Atlas mountainous catchments of Morocco. Nat Hazards 86(2):953–967